J. Marine Sci. Appl. (2015) 14: 208-214
DOI: 10.1007/s11804-015-1293-y

Morphological Research on Geometrical Scattering Waves of an Underwater Target

Xiukun Li[1,2*], Mingye Liu[1,2] and Shu Jiang[1,2]

1. Acoustic Science and Technology Laboratory, Harbin Engineering University, Harbin 150001, China
2. College of Underwater Acoustic Engineering, Harbin Engineering University, Harbin 150001, China

Abstract: In this paper, a new method based on morphologic research named reconstruction cross-component removal (RCCR) is developed to analyze geometrical scattering waves of an underwater target. Combining the origin of the cross-component in Wigner-Ville distribution, the highlight model of target echoes and time-frequency features of linear frequency-modulated signal can remove cross-components produced by multiple component signals in Wigner-Ville distribution and recover the auto-components of output signals. This method is used in experimental data processing, which can strengthen the real geometric highlights, and restrain the cross components. It is demonstrated that this method is helpful to analyze the geometrical scattering waves, providing an effective solution to underwater target detection and recognition.
Keywords: underwater target detection; geometrical scattering waves; Wigner-Ville distribution; morphology; reconstruction cross-component removal (RCCR)

Article ID: 1671-9433(2015)02-0208-07

1 Introduction

Underwater target detection and recognition technology is one of the current research focuses in underwater acoustic field. For bottom and buried targets, detection and recognition technology is mostly based on active sonar. With the development of electronic and information processing technology, feature extraction, feature fusion and classification decision based on signal space become three core techniques of active sonar detection and recognition (Li and Xia, 2013). Currently, researches in this field focus on physical characteristics and signal features of target, reverberation field and anti-reverberation techniques. Because of the important theoretical and practical value of target echo, many scholars have conducted wide and deep studies on it. Target echo is also known as monostatic scattering, it refers to the reverse scattering wave from the target. Fan (2001) studied the echo characteristics of underwater complex targets. Fan *et al.* (2010) studied the scatting sound field structure of water-filled cylindrical shell. The acoustic scattering from a finite periodically or quasi-periodic bulkhead cylindrical shell was studied by Pan *et al.* (2012, 2013a, 2013b, 2014). Besides, the scattering of obliquely incident plane waves by cylindrical shells immersed in water was measured by Scot *et al.* (1997) and the ray methods (Florian and Philip, 2002) was developed to model and interpret those responses. Ying *et al.* (2003) investigated the circumferential resonance modes in such condition. The resonance scattering theory can provide the physical explanations for observations (Mitri, 2010; Farhang *et al.*, 2011). Williams *et al.* (2010) researched the sound scatting of a solid cylinder half-buried in sand. The scattering of fully buried target was studied by Waters *et al.* (2012). These work illustrated the physical mechanism and signal properties of acoustic scattering from different underwater targets. The scattering waves can represent the characteristics of underwater target. Li *et al.* (2010) studied the feature extraction and fusion based on the characteristics of underwater target. In order to deal with the limitations of underwater target feature extraction, Sun and Li (2013) proposed a method based on empirical mode of decomposition and Wigner-Ville distribution (WVD) to extract the highlight features of a small underwater target, which is proved to be effective in underwater target recognition.

Mathematical morphology originally took shape in 1960s, for about 60 years, its application has expended to image, video, mechanics and many other fields. The theory of morphology can be applied to many aspects of image processing, for instance, target recognition, image reconstruction, *etc*. As a new image processing method, it has been used in image analysis and processing fields. For underwater acoustic area, Liu and Sang (2003) proposed an underwater acoustic image processing method based on mathematical morphology.

In this paper, reconstruction cross-component removal (RCCR) (Soledad *et al.*, 2011) based on morphological reconstruction is applied to process target echo. Short-time Fourier transform and Wigner-Ville distribution are combined and used in a new way to analyze highlight structure of underwater target echo.

Received date: 2014-07-18.
Accepted date: 2014-10-08.
Foundation item: Supported by the National Natural Science Foundation of China, under Grant No.51279033 and the Natural Science Foundation of Heilongjiang Province, China, under Grant No. F201346.
***Corresponding author Email:** lixiukun@hrbeu.edu.cn

2 Features of target echo

In order to obtain the features of target echo, analysis in time domain and frequency domain are necessary. Since underwater target echo is a type of non-stationary signal, it needs to be described in both time and frequency domains, i.e., using joint function to show the features of underwater target echo. In this paper, short time Fourier transform (STFT) and Wigner-Ville distribution (WVD) are applied.

2.1 Target model in this paper

According to the theory of highlight model (Tang, 1994), the transfer function for single highlight is

$$\boldsymbol{H}_m(\boldsymbol{r},\omega)=\boldsymbol{A}_m(\boldsymbol{r},\omega)\mathrm{e}^{\mathrm{i}\omega\tau_m}\mathrm{e}^{\mathrm{i}\varphi_m} \tag{1}$$

where $\boldsymbol{A}_m(\boldsymbol{r},\omega)$ is the amplitude factor; τ_m is time delay, which is determined by the distance between the equivalent scattering center and the reference point, together with a function of azimuth angle θ; φ_m is the phase jump that is produced when the echo forms. In this case, the transfer function of the target which has N highlights can be described as:

$$\boldsymbol{H}(\boldsymbol{r},\omega)=\sum_{m=1}^{N}\boldsymbol{A}_m(\boldsymbol{r},\omega)\mathrm{e}^{\mathrm{i}\omega\tau_m}\mathrm{e}^{\mathrm{i}\varphi_m} \tag{2}$$

In this paper, the target model is a cylinder with semi-spherical head, as shown in Fig. 1. According to acoustic scattering features of the target, this target model can be divided into a spherical crown and a cylinder. To get this target echo highlight model, highlight parameters of the two components, spherical crown and cylinder with limited length, need to be studied. Highlight parameters of sphere and cylinder are shown in Tables 1 and 2, respectively.

In order to analyze the geometrical highlight structure of target echo, echo types concerned in this paper include mirror-reflection wave and edge wave (elastic wave was not concerned in this paper).

During the experiment, incident sound wave reached the target model horizontally. Therefore, the wave front paralleled to the rotational axis of the target model's azimuth angle. It should be noted that when θ equaled to certain values, highlights might be in the shadow zone. In this case, not all the highlights could appear at the same time. Highlights from mirror reflection appeared at abeam, end and spherical crown, and highlights at abeam and end only appeared when the sound wave reached the target model vertically. In other words, when $\theta=0°$ and $\theta=360°$, mirror reflection highlights appeared at end; when $90°<\theta<270°$, highlights appeared at spherical crown. Since the rotating range of the target model was 0°–360°, the relation of highlight position and the incident angle is illustrated in Table 3.

When the relationship between locations of highlights and the angle of incident sound wave is known, the transform function can be calculated. The time delay (from the reference center) is a necessary parameter of each highlight. In accordance to the water tank experiment, the rotational center (i.e. the center of the cylinder part) of the target was selected to be the reference center *O*. Assuming that far field condition was met, the sound wave arrived at the surface of the target could be considered as plane wave. Therefore, time delay of each highlight could be obtained, as listed in Table 4.

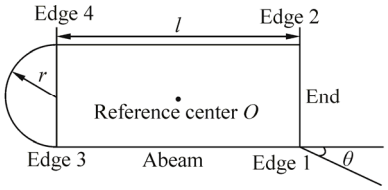

Fig. 1 The target model

Table 1 Highlight parameters of sphere

Highlight	$\boldsymbol{A}_m$	τ_m	φ_m
Specular reflection	$r/2$	$-2r/c$	0

Table 2 Highlight parameters of cylinder

Highlight	$\boldsymbol{A}_m$	τ_m	φ_m
Edge1	$\frac{r}{4\pi}\sqrt{\frac{\pi}{kr}}\frac{1}{\sin^{3/2}\theta\cos\theta}$	0	$\frac{\pi}{4}$
Edge2	$\frac{r}{4\pi}\sqrt{\frac{\pi}{kr}}\frac{\cos\theta}{\sin^{3/2}\theta}$	$\frac{4r\sin\theta}{c}$	$\frac{3\pi}{4}$
Edge3	$\frac{r}{4\pi}\sqrt{\frac{\pi}{kr}}\frac{\sin^{1/2}\theta}{\cos\theta}$	$\frac{2l\cos\theta}{c}$	$\frac{5\pi}{4}$

Table 3 Relation of highlight position and incident angle

Angle	Highlight position
$\theta=0°$	End, Edge 1, 2
$0°<\theta<90°$	Edge 1, 2 and 3
$\theta=90°$	Abeam, Edge 1, 3
$90°<\theta<180°$	Spherical crown, Edge 1, 3
$\theta=180°$	Spherical crown, Edge 3, 4
$180°<\theta<270°$	Spherical crown, Edge 2, 4
$\theta=270°$	Abeam, Edge 2, 4
$270°<\theta<360°$	Edge 1, 2 and 4
$\theta=360°$	End, Edge 1, 2

Table 4 Time delay of highlights

Highlight	Time delay
Edge 1	$-2\sqrt{\left(\frac{l}{2}\right)^2+r^2}\cos\left[\theta-\arctan\left(\frac{2r}{l}\right)\right]\Big/c$
Edge 2	$-2\sqrt{\left(\frac{l}{2}\right)^2+r^2}\cos\left[\theta+\arctan\left(\frac{2r}{l}\right)\right]\Big/c$
Edge 3	$2\sqrt{\left(\frac{l}{2}\right)^2+r^2}\cos\left[\theta+\arctan\left(\frac{2r}{l}\right)\right]\Big/c$
Edge 4	$2\sqrt{\left(\frac{l}{2}\right)^2+r^2}\cos\left[\theta-\arctan\left(\frac{2r}{l}\right)\right]\Big/c$
Spherical Crown	$-2\left[r+\frac{l}{2}\cos(\pi-\theta)\right]\Big/c$
Abeam	$-\frac{2r}{c}$

2.2 Cross component of WVD

In this paper, linear frequency-modulated (LFM) signal was selected to be the emitting signal in experiment.

Assuming the amplitude of single component LMF is 1, denoted as $z(t)=\exp\left[\mathrm{j}2\pi\left(f_0 t+\frac{1}{2}mt^2\right)\right]$, the quadratic form of it is

$$\begin{aligned} &z(t+\frac{\tau}{2})z^*(t-\frac{\tau}{2})= \\ &\exp\left\{\mathrm{j}2\pi\left[f_0(t+\frac{\tau}{2})+\frac{1}{2}m(t+\frac{\tau}{2})^2\right]\right\}\cdot \\ &\exp\left\{-\mathrm{j}2\pi\left[f_0(t-\frac{\tau}{2})+\frac{1}{2}m(t-\frac{\tau}{2})^2\right]\right\} \end{aligned} \tag{3}$$

Then its WVD is

$$\begin{aligned} &W_z(t,f)=\int_{-\infty}^{+\infty}z(t+\frac{\tau}{2})z^*(t-\frac{\tau}{2})\mathrm{e}^{-\mathrm{j}2\pi f\tau}\,\mathrm{d}\tau= \\ &\int_{-\infty}^{+\infty}\mathrm{e}^{\mathrm{j}2\pi\tau(f_0+mt)}\mathrm{e}^{-\mathrm{j}2\pi f\tau}\,\mathrm{d}\tau=\delta[f-(f_0+mt)] \end{aligned} \tag{4}$$

For a complex harmonic signal with amplitude 1, i.e. $z(t)=\mathrm{e}^{\mathrm{j}\omega_1 t}+\mathrm{e}^{\mathrm{j}\omega_2 t}$, its WVD is

$$\begin{aligned} &W_z(t,\omega)=W_{\mathrm{auto}}(t,\omega)+W_{\mathrm{cross}}(t,\omega)= \\ &W_{z_1}(t,\omega)+W_{z_2}(t,\omega)+2\,\mathrm{Re}[W_{z_1,z_2}(t,\omega)] \end{aligned} \tag{5}$$

In which the auto-component is,

$$\begin{aligned} &W_{\mathrm{auto}}(t,\omega)=W_{z_1}(t,\omega)+W_{z_2}(t,\omega)= \\ &2\pi[\delta(\omega-\omega_1)+\delta(\omega-\omega_2)] \end{aligned} \tag{6}$$

And the cross-component is,

$$\begin{aligned} &W_{z_1,z_2}(t,\omega)=\int_{-\infty}^{+\infty}\exp[\mathrm{j}\omega_1(t+\frac{\tau}{2})-\mathrm{j}\omega_2(t-\frac{\tau}{2})]\exp(-\mathrm{j}\omega\tau)\mathrm{d}\tau= \\ &\exp[(\omega_1-\omega_2)t]\int_{-\infty}^{+\infty}\exp[-\mathrm{j}(\omega-\frac{\omega_1+\omega_2}{2})\tau]\mathrm{d}\tau= \\ &2\pi\delta(\omega-\omega_m)\exp(\omega_d t) \end{aligned} \tag{7}$$

If the signal has multiple components, cross-components will be introduced by dot product calculation. No matter how far the components are from each other in time-frequency plane, WVD cross components always exist, and have serious effect.

3 Morphological reconstructions

If the morphological information of auto-components can be gained by processing STFT, morphological theory can be used on WVD to remove cross-components and keep auto terms. In this paper, morphological reconstruction is applied to solve this issue.

3.1 Erosion and dilation

Erosion and dilation are two primary operations of morphological processing (Zhu, 2013). To understand the morphological method used in this paper, a brief introduction of these two operations is included.

With A being the image set and B a structuring element, the erosion of A by B, denoted as $A\Theta B$, is

$$A\Theta B=\{z\in Z^2\mid z+b\in A,\forall b\in B\} \tag{8}$$

or

$$A\Theta B=\{z\in Z^2\mid B_z\subseteq A\} \tag{9}$$

or

$$A\Theta B=\bigcap_{b\in B}A_{-b} \tag{10}$$

The equation indicates that the erosion of A by B is the set of the points in A that the point z passes through when B shifts in A, where z is a given point in B.

Fig. 2 is an example of erosion, A is a solid square with length d, structuring element B_1 is a square with length $d/3$, and B_2 is a rectangle with length d and width $d/3$. Both B_1 and B_2 have an origin, respectively. From the result of erosion, $A\Theta B_1$ is a square with length $2d/3$, and $A\Theta B_2$ is a straight line.

As for dilation, with A being the image set and B a structuring element, the dilation of A by B, denoted as $A\oplus B$, is defined as,

$$A\oplus B=\{z\in Z^2\mid z=a+b,a\in A,b\in B\} \tag{11}$$

or

$$A\oplus B=\{z\in Z^2\mid[\hat{B}_z\cap A]\subseteq A\} \tag{12}$$

or

$$A\oplus B=\bigcup_{b\in B}A_b \tag{13}$$

where $\hat{B}_z=\{z\in Z^2\mid z=-b,b\in B\}$.

The equation of dilation is based on reflecting B about its origin. The dilation of A by B then is the set of the area that B passes through when a base point in B shifts in A, such that B and A overlap by at least one element.

Similar to Fig. 2, Fig. 3 is an example of dilation. The results show that $A\oplus B_1$ is a square with width $4d/3$, and $A\oplus B_2$ is a rectangle with length $2d$ and width $4d/3$.

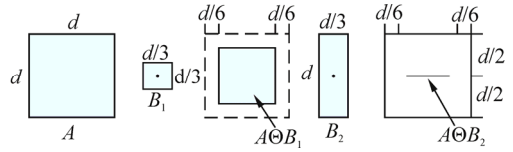

Fig. 2 Erosion of A by B_1 and B_2

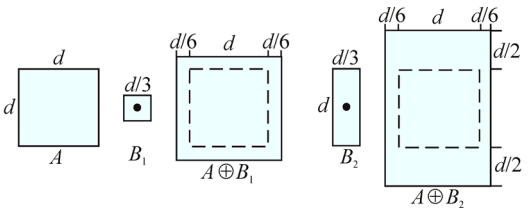

Fig. 3 Dilation of A by B_1 and B_2

3.2 Morphological reconstruction method

This method involves two images and a structuring element. One image, the marker, contains the starting points for the transformation; the other image, the mask, constrains the transformation. The structuring element is used to define connectivity.

Central to morphological reconstruction are geodesic dilation and geodesic erosion. Using f to denote the marker image and g the mask image, the geodesic dilation of size 1 of the marker image with respect to the mask is denoted by $\delta_g^{(1)}(f)$. Geodesic dilation is to compare the marker image g and the dilation of the marker image $\delta^{(1)}(f)$, and extract the smallest value of each point,

$$\delta_g^{(1)}(f) = \delta^{(1)}(f) \wedge g \tag{14}$$

and geodesic erosion is,

$$\begin{aligned} \varepsilon_g^{(1)}(f) &= [\delta^{(1)}(f^c) \wedge g^c]^c = \\ [(\varepsilon^{(1)}(f))^c \wedge g^c]^c &= \varepsilon^{(1)}(f) \vee g \end{aligned} \tag{15}$$

where $\varepsilon^{(1)}$ denotes erosion. Geodesic erosion completes erosion operation of the marker image, then it is compared with the marker image and the biggest value of each point is derived.

The positions of auto terms of WVD and STFT are almost the same and the morphology of auto terms are similar. According to morphological reconstruction, STFT can be used as the marker image and WVD the mask image. Additionally, the image features from WVD and STFT are processed with dilation reconstruction method.

The process of RCCR method is illustrated as Fig. 4. The major idea of this method is to extract auto items of the signal from WVD and reconstruct it, and then remove cross components to reduce its influence on auto items.

In order to make the result of morphological reconstruction more accurate, pre-process is necessary after STFT. This pre-process is to conduct threshold segmentationand homotopic thinning on the STFT result. Therefore, morphological structure information of STFT could be obtained and marker image f is available. On the other hand, WVD of input signal is used as mask image g. In this way, STFT's time-frequency resolution was improved and ensured that positions of auto items are the same in WVD and STFT.

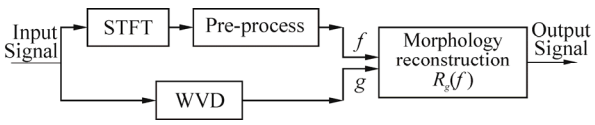

Fig. 4 The schematic diagram of Reconstruction cross-component removal (RCCR)

4 Experiments

An experiment is conducted in an anechoic tank to collect the acoustic scattering waves from a target model. The size of the tank is 25 m long, 15 m wide and 10 m deep. The equipment of the experiment is shown in Fig. 5.

A monostatic sonar array is used to transmit and receive signal. The LFM pulse is used as transmitted signal. The data collection synchronizes with transmitting signal, so the time delay will be measured exactly. The target model is a cylinder with semi-spherical head, which is hung by ropes to a rotating stent. In the experiment, the target model rotates horizontally, which can achieve the acoustic scattering waves under different incident angles. Best efforts are made to ensure that the array and target model are in the same depth and the target rotate uniformly.

For all the data obtained in the experiment, the pulse width and frequency range are normalized. The position of the target and the direction of incident sound wave in any angle θ are shown as Fig. 6.

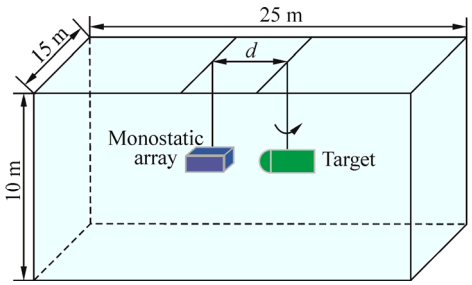

Fig. 5 Experiment equipment

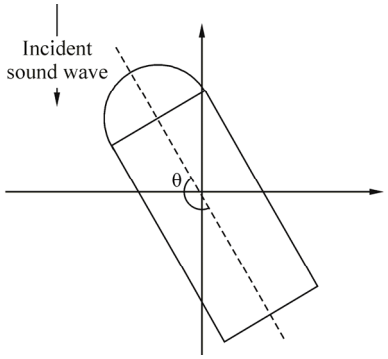

Fig. 6 Target direction and incident sound wave

4.1 Energy distribution of target echo

It is assumed that the distance between the source and the target meets the far field condition. In the experiment, the monostatic array is static (i.e., the direction of incident sound wave did not change), and the target completes counterclockwise rotation with uniform velocity, meanwhile echo data is recorded.

The actual target echo energy distribution is drawn by using echo data obtained in experiment, as shown in Fig. 7. The change of each highlight echo with rotation angle can be observed. Comparing data in Tables 3 and 4, it is clear that the energy distribution of theoretical and experiment echoes have similar change tendency. In other words, theoretical positions where mirror-reflection wave and edge wave of the target echo's geometric highlight structure should appear are proved by experiment.

However, this image cannot fully present the features of

target echo. In actual experiment, multiple interfering lines might appear in echo energy distribution figure. For instance, the reflection echo lines of the rope and hook used to hang the target or other objects exist here. In this case, it is difficult to determine which track it was from the real target echo.

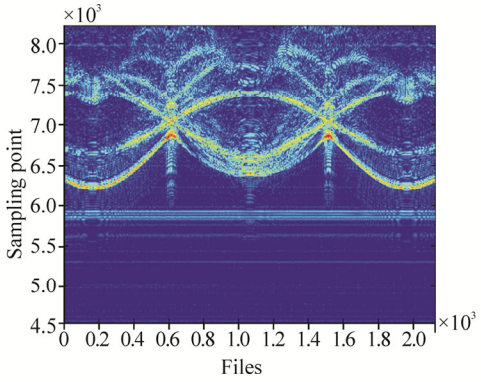

Fig. 7 Actual echo energy distribution

4.2 Cross components removal

Based on target echo energy distribution obtained in the experiment, the RCCR method is used to extract geometric highlights of target echo. The results are shown as below.

According to the waveform files got at angle θ_1, time domain waveform and matched filtering of all the basic elements in the receiving array are calculated. Comparing the calculated results and actual working situation of basic elements in the experiment, data of an element channel is selected to be processed.

The scattering wave received by this channel is shown in Fig. 8. Fig. 8(a) shows the original data in the time domain without any processing and Fig. 8(b) shows the frequency spectrum after normalization. The data between sampling points [6 500, 8 500] in original oneof the target echo data is intercepted and used as the input data for RCCR later.

According to RCCR method, the first step is to conduct STFT on signal, and the result is shown as Fig. 9(a), then conduct pre-process on the outcome of STFT, the result is shown as Fig. 9(b). The result obtained after STFT and pre-process is the marker image in morphological reconstruction process. From Fig. 9(b), the marker image contents only one slant.

The following step is to calculate WVD of the data and the result is shown as Fig. 10(a), which is used as the mask image in RCCR. From Fig. 10(a), a line spectrum with relatively high brightness can be observed, beside which there are a few slants with less energy. The darker line spectrum results from reflection of the rope. By using the mask and marker image, RCCR process can be completed and the result is shown as Fig. 10(b). Compared with Fig. 10(a), the outline of processed result is narrower and only one bright line spectrum is kept, which proved that noise and reflection of rope echo are filtered. Also, the geometric highlights of target echo are strengthened.

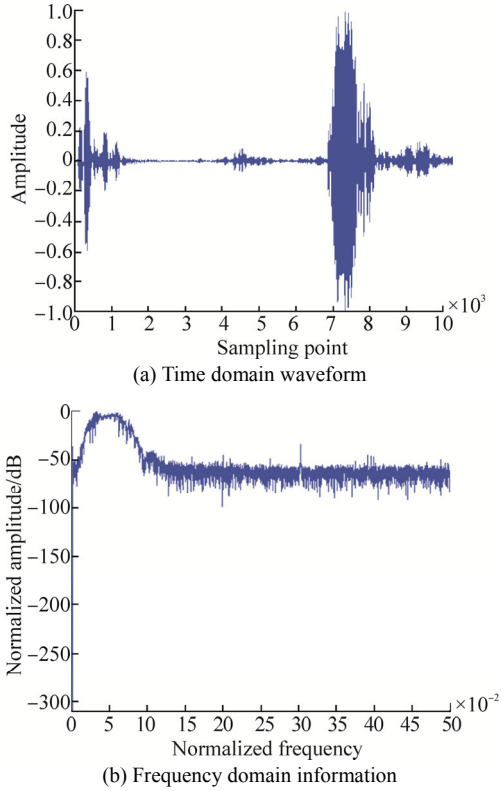

Fig. 8 Signal received by the element

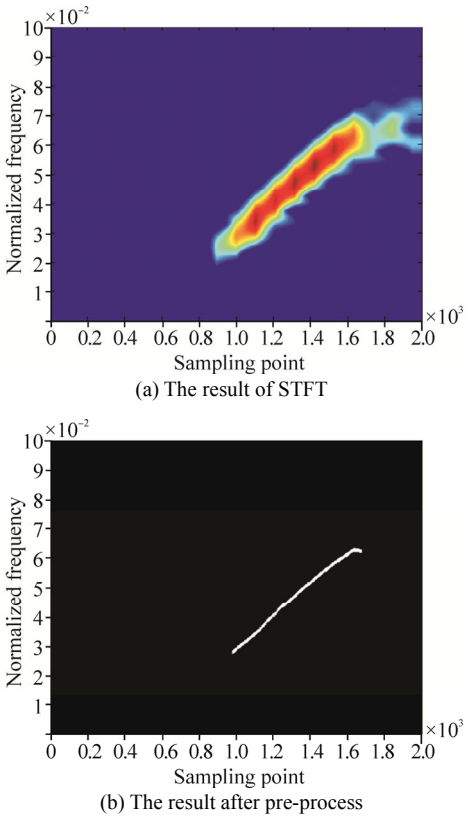

Fig. 9 The results of STFT and pre-process

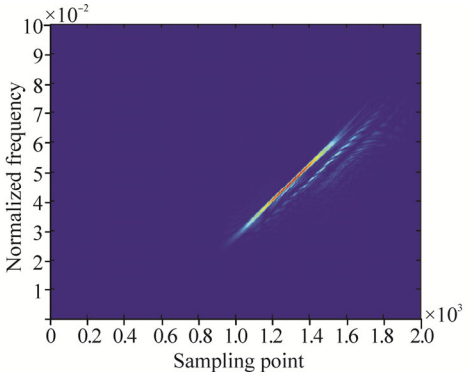

(a) The result of STFT

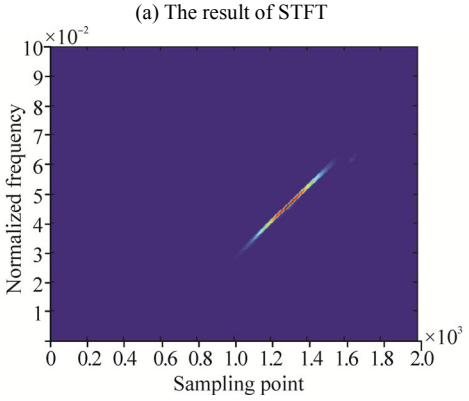

(b) The result after processing

Fig. 10 The results before and after processing

Additionally, the processing result shows clearly that there is a highlight with more energy, then it can be determined that the target model is abeam. Based on the original position of the target and selected files, calculation proves that conclusion is correct. In other words, at angle θ_1, RCCR is proved to be functioning.

Besides experiment at angle θ_1, two more experiments at different angles are conducted. All three experiments prove that RCCR works well at different angles.

5 Conclusions

The acoustic scattering waves of an underwater target usually consist of multiple components. In some time-frequency distributions with high resolution, such as Wigner-Ville distribution, the cross-componentscan lead to difficulty in analysis. Combining morphological image processing and time-field analysis of signal, this paper applies RCCR method to underwater target echo analysis. This method is not only able to detect target echo, but also strengthen the real geometric highlights and restrain the cross components in WVD and other interferes. Introducing morphological image processing methods into the underwater acoustic field provides a possible direction in solving underwater target detection and recognition issues.

For future work, CW pulse may be selected as emitting signal. Since only LFM is discussed in this paper, whether RCCR method can be used for CW pulse or other types of signal is to be studied.

References

Fan J (2001). *Study on echo characteristics of underwater complex targets*. PhD thesis, Shanghai Jiao Tong University, Shanghai. (in Chinese)

Fan W, Zheng GY, Fan J (2010). Analysis of circumferential waves on a water-filled cylindrical shell. *Acta Acoustica*, **35**(4), 419-426. (in Chinese)

Farhang H, Esmaeil E, Anthony NS (2011). Correlation between helical surface waves and guided modes of an infinite immersed elastic cylinder. *Ultrasonics*, **51**(2), 238-244.
DOI: 10.1016/j.ultras.2010.08.008

Florian JB, Philip LM (2002). Leaky helical flexural wave backscattering contributions from titled cylindrical shells in water: Observations and modeling. *The Journal of the Acoustical Society of America*, **112**(2), 528-536.
DOI: 10.1121/1.1492822

Li XK, Li TT, Xia Z (2010). Feature extraction and fusion based on the characteristics of underwater targets. *Journal of Harbin Engineering University*, **31**(7), 903-908. (in Chinese)
DOI: 10.3969/j.issn.1006-7043.2010.07.014

Li XK, Xia Z (2013). Research of underwater bottom object and reverberation in feature space. *Journal of Marine Science and Application*, **12**(2), 235-239.
DOI: 10.1007/s11804-013-1190-1

Liu CC, Sang EF (2003). Underwater acoustic image processing based on mathematical morphology. *Journal of Jilin University (Information Science Edition)*, **21**(5), 52-57. (in Chinese)

Mitri FG (2010). Acoustic backscattering enhancements resulting from the interaction of an obliquely incident plane wave with an infinite cylinder. *Ultrasonics*, **50**(7), 675-682.
DOI: 10.1016/j.ultras.2010.01.005

Pan A, Fan J, Wang B (2013a). Acoustic scattering from a double periodically bulkheaded and ribbed finite cylindrical shell. *The Journal of the Acoustical Society of America*, **134**(5), 3452-3463.
DOI: 10.1121/1.4821212

Pan A, Fan J, Wang B, Chen ZG, Zheng GY (2014). Acoustic scattering from the finite periodically ribbed two concentric cylindrical shells. *Acta Physica Sinica*, **63**(21), 024301. (in Chinese)
DOI: 10.7498/aps.63.214301

Pan A, Fan J, Zhuo LK (2012). Acoustic scattering from a finite periodically bulkhead in cylindrical shell. *Acta Physica Sinica*, **61**(21), 214301. (in Chinese)
DOI: 10.7498/aps.61.214301

Pan A, Fan J, Zhuo LK (2013b). Acoustic scattering from a finite quasi-periodic bulkhead cylindrical shell. *Acta Physica Sinica*, **62**(2), 024301. (in Chinese)
DOI: 10.7498/aps.62.024301

Scot FM, Philip LM, Gregory K (1997). High-frequency backscattering enhancements by thick finite cylindrical shells in water at obliquely incidence: Experiments, interpretation, and calculation. *The Journal of the Acoustical Society of America*, **103**(2), 785-794.
DOI: 10.1121/1.421200

Soledad G, Valery N, Ramón M (2011). Removing interference components in time-frequency representations using morphological operators. *Journal of Visual Communication and Image Representation*, **22**(5), 401-410.
DOI: 10.1016/j.jvcir.2011.03.007

Sun SJ, Li XK (2013). Underwater target feature extraction using empirical mode decomposition and WVD method. *Journal of Harbin Engineering University*, **34**(8), 967-971. (in Chinese) DOI: 10.3969/j.issn.1006-7043.201303021

Tang WL (1994). Highlight model of echoes from sonar targets. *Acta Acustica*, **19**(2), 92-100. (in Chinese)

Waters ZJ, Simpson HJ, Sarkissian A, Dey S, Houston BH, Bucaro JA, Yoder TJ (2012). Bistatic, Above-critical angle scattering measurements of fully buried unexploded ordnance (UXO) and clutter. *The Journal of the Acoustical Society of America*, **132**(5), 3076-3085. DOI: 10.1121/1.4757098

Williams KL, Kargl SG, Thorsos EI, Burnett DS, Lopes JL, Zampoli M, Marston PL (2010). Acoustic scattering from a solid aluminum cylinder in contact with a sand sediment: Measurements, modeling, and interpretation. *The Journal of the Acoustical Society of America*, **127**(6), 3356-3371. DOI: 10.1121/1.3419926

Ying F, Farhang H, Anthony NS, Mohammad-Reza J (2003). Circumferential resonance modes of solid elastic cylinders excited by obliquely incident acoustic waves. *The Journal of the Acoustical Society of America*, **113**(1), 102-113. DOI: 10.1121/1.1525289

Zhu X (2013). *Target echo detection based on time-frequency analysis and image morphology*. M.E. thesis, Harbin Engineering University, Harbin. (in Chinese)

Underwater Technology Conference 2015

June 17–18, 2015,
Bergen, Norway

The Underwater Technology Conference (UTC 2015) has a well-known history of presenting highly competent speakers on current and important topics for the subsea industry. UTC 2015 will be the 21th Underwater Technology Conference in Bergen, and 900 professionals and 60 exhibitors are expected to attend the conference.

The subsea industry is under pressure from both market and nature. High costs and reduced operating margins are forcing operators to shelve and postpone projects. Deep waters, high reservoir pressures and need for boosting and compression requires effective and efficient solutions. We believe a step change in innovation, standardization and collaboration is required to obtain significant cost reductions and enable a new wave of projects and prolonged production. We trust you wish to contribute to a thriving industry for the future, and the UTC Program Committee invite you to submit your abstract.

The Program Committee have received a record number of abstracts for evaluation for UTC 2015. This shows that UTC is more relevant than ever as an arena for sharing of knowledge and discussions of new solutions. We are very pleased with the great response to "Subsea under pressure-innovating for the next wave". All authors will be notified by the end of February, and the program for UTC2015 will be published by the end of March.

We look forward to inviting you all to Bergen for the 21st Underwater Technology Conference (16) 17- 18 June!

Topics of interest at UTC 2015

- **Technological innovations—Control, Power and Instrumentation**
  - Components
  - Units
  - Systems
  - Concepts
- **Technological innovations—Materials, Mechanical and Marine disciplines**
  - Components
  - Units
  - Systems
  - Concepts
- **Field Development Concepts and Experiences**
  - Production
  - Processing
  - Umbilicals
  - Risers
  - Pipelines
- **Simplification, Standardization and Enhanced Industry Collaboration**
  - Production—equipment and systems
  - Processing—equipment and systems
  - Pipelines—equipment and systems
  - Umbilicals
  - Risers
  - New contractual strategies
- **Improved Asset Value and Significant Cost Reductions**
  - Brownfield rejuvenation
  - Lifetime extension
  - Effective and efficient installation and intervention
  - Field operational experiences
  - New repair methods

Website: http://www.utc.no/conference/